ELSEVIER

Journal of Power Sources 96 (2001) 369–375

JOURNAL OF POWER SOURCES

www.elsevier.com/locate/jpowsour

The role of electrodes in power degradation of AMTEC: analysis and simulation

M.A.K. Lodhi[a,*], M.S. Chowdhury[b]

[a]*Department of Physics, Texas Tech University, Lubbock, TX 79409, USA*
[b]*Department of Chemical Engineering, Texas Tech University, Lubbock, TX 79409, USA*

Received 25 October 2000; accepted 8 November 2000

Abstract

During the testing of the alkali metal thermal to electric converter (AMTEC) in laboratory, maximum power output of the AMTEC was found to be decreasing from 2.48 to 1.27 W after 18,000 h of operation with the hot side temperature of 1023 K and the condenser side temperature of 600 K. Electrode is one of the components in AMTEC which has effective lifetime. In this study, the role of the electrode on the overall power degradation has been investigated and reasons of the degradation are established qualitatively and quantitatively. The electrode is found 17% on average responsible for the overall degradation of power output. © 2001 Elsevier Science B.V. All rights reserved.

Keywords: AMTEC; Electrode; Power degradation; Time dependency; Grain growth

1. Introduction

In 1962, Ford Motor Company first used thermally powered sodium concentration cells in the development of sodium sulfur battery based on the unique electrical properties of beta-alumina solid electrolyte (BASE). This new device was called sodium heat engine [1] or alkali metal thermal to electric converter (AMTEC). It was the first device with high efficiency and power density to be competitive with conventional heat engine [2].

Direct solid-state converters have been used in space missions for quite a long-time. But they have at-least one limitation of low conversion efficiency. The AMTEC provides all the potential benefit of the solid-state conversion devices plus an edge over other solid-state converters by providing high efficiency almost close to the Carnot efficiency [3].

The AMTEC offers high thermal to electric efficiency, high reliability, and no noise. It has no moving parts with the resulting potential for low maintenance and high durability, and ability to use heat energy as an input from the high temperature combustion, nuclear, solar or radio-isotope [4,5]. As it has no moving parts, after start up of power system, it is not subject to any material wear and tear. There are no vibration or uncompensated momentum present in AMTEC, which reduces the chances of corrosion. The AMTEC has a modular construction. If any one of the parts fails, only that part of the device is affected, which is an added reliability of the system. The AMTEC offers a great advantage in system design. The hot side temperature range makes it compatible to connect with other conversion systems. For example, hot temperature side of AMTEC can be coupled with the heat rejection side of thermionic converters or with solid oxide fuel cells (SOFC) operating at 1273 K [6]. It can also use the waste heat from the high temperature emitters of the thermo-photo-voltaic converters [7–9].

The AMTEC is being used for building gas fired power systems [6]. It has also applications in field operation [6]. For instance, it can be used as a portable power system in remote site applications, cogeneration units, self powered furnaces, rechargeable batteries, cross-county trucking, etc. [10]. It has uses as power systems of recreational vehicles, transportation, communication relay stations, weather buoys, vacation homes, construction sites, and military applications [11]. Using only 500 g of sodium, it is possible to produce 20 kW of power by AMTEC [12].

Recently, much of the development of AMTEC has been done relating to space power. During the extended testing of the AMTEC, maximum power output of the AMTEC was found to be decreasing from 2.48 to 1.27 W after 18,000 h of operation with the hot side temperature of 1023 K and the

* Corresponding author. Tel.: +1-806-742-3778; fax: +1-806-742-1182.
E-mail address: b5mak@ttacs.ttu.edu (M.A.K. Lodhi).

0378-7753/01/$ – see front matter
PII: S0378-7753(00)00667-4

condenser side temperature of 600 K. Electrode is one of the most degrading components in the AMTEC. In this study, the role of the electrode in the power degradation has been investigated. An 18,000 line FORTRAN code has been used to simulate and analyze the transient behavior of AMTEC. This FORTRAN code is based on four principle models, namely, (1) vapor pressure loss model, (2) electrochemical model, (3) thermal model, and (4) electrical model.

Vapor pressure loss model calculates the sodium vapor pressure at the interface of cathode and BASE as a function of temperature and sodium vapor flow rate [13–16]. Electrochemical model calculates the voltage differential across the BASE as a function of cell electric current, external load resistance, BASE and condenser temperature, and sodium pressure differential across the BASE [13,14,16–18].

Thermal model calculates heat conduction in the cell structure and thermal radiation exchanges among all surfaces within the cell cavities. The model calculates radiation and conduction heat fluxes between the different elements of the cell [13,16]. Electrical model calculates the electrical resistance of the both BASE and current collectors, the cell internal resistance, and total electrical current as a function of the external load resistance [13,16]. The description of these models can be found in the work of M.S. Chowdhury [13].

The given FORTRAN code was written for steady-state analysis of AMTEC. The program has been modified in this study to deliver both the steady-state and transient analysis of AMTEC in the same time. For the transient analysis, a variable time-step has been taken from 0 to 130,000 h (approximately 15 years). The program is able to calculate and display grain size, temperature independent exchange current, power output, and time given the relation between grain size with time and temperature independent exchange current with grain size.

2. Working principle of the AMTEC

We describe the working principle of AMTEC with special reference to its design version PX-3A whose parameters we have used for this study. The AMTEC is a thermally regenerative electrochemical concentration cell for the direct conversion of heat to electrical energy without the use of moving mechanical parts [2–4,6]. It uses liquid sodium as a working fluid and a solid electrolyte as an ionic conductor through which a nearly isothermal expansion of sodium can generate high current/low voltage power at high efficiency. This heat engine is based on the unique properties of BASE that is an excellent ionic conductor but a poor electron conductor.

The BASE is a dense micro-crystalline sintered ceramic ($Na_{5/3}Li_{1/3}Al_{32/3}O_{17}$) which divides the AMTEC (PX-3A) into two regions, a heated region filled with sodium at high-pressures (10–100 kPa) and high-temperatures (900–1300 K) and a cooled sodium vapor region at low-pressures (<50 Pa) and low-temperatures (400–700 K) [19]. The BASE conducts only sodium ions but not neutral sodium or electrons. A porous metal electrode (cathode) covers the low-pressure (outer) side of the BASE. The anode surface covers the inner side of the BASE at the high pressure-temperature region of the cell (see Fig. 1). Both electrodes

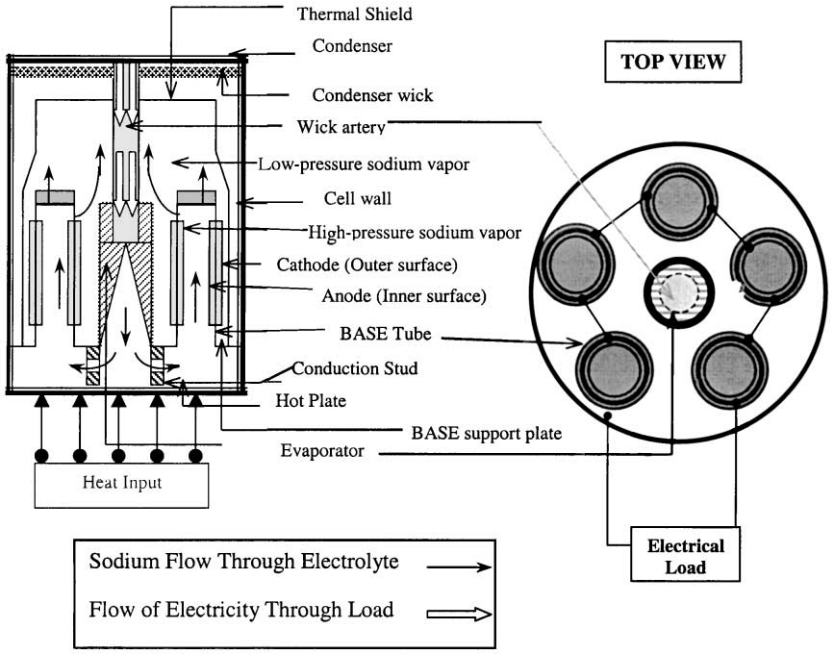

Fig. 1. Cross and top sectional views of the PX-3A cell.

provide a conduction path for the electrons to and from the external load. Sodium at temperature, T_1 enters the hot region of the cell and absorbs externally supplied energy until it reaches a temperature T_2. Due to the thermodynamic potential across the BASE, ionization of sodium metal occurs at the hot region of sodium and BASE interface. The following reaction occurs at the interface of BASE and anode electrode surface [11]:

$$\mathrm{Na\,(vapor)} \rightarrow e^- + [\mathrm{Na}^+] \tag{1}$$

The sodium ions are diffused through the BASE to the cathode due to the pressure differential across the BASE. The electrons circulate through the external load producing electrical work and then reach the cathode surface where they recombine with the sodium ions at the interface between the BASE and cathode.

The following reaction occurs at the interface of BASE and cathode electrode surface [11]:

$$e^- + [\mathrm{Na}^+] \rightarrow \mathrm{Na\,(vapor)} \tag{2}$$

The neutralized sodium leaves the porous electrode, moves through the vapor space, and releases their heat of condensation on the condenser surface at T_1. Nearly the entire temperature drop occurs in this low-pressure vapor space. The condensed liquid sodium moves to the wick annulus to the inlet of a small dc electromagnetic pump or a porous capillary wick, which is used to return the sodium to the high-pressure evaporator region. The BASE tube temperature is kept slightly higher than that of evaporator to prevent condensation of sodium in the anode cavity [16,19].

3. Time dependent theoretical solution of power output

The focused simulation studies have been on the transient behavior of the surface self-diffusion and grain growth effect of electrode material. As the grains sinter, they coalesce, reduce the operable area of the electrode and increase the size of the grain. But as the grain size increases, void in the electrode increases which lead to less contact between the electrode and electrolyte which, again leads to the higher resistivity and lower conductivity in the electrode.

The modeling of grain growth by Ryan et al. [20] is used in this study in order to find out the grain growth of TiN electrode. The equation for grain growth is given by [20]

$$R_\mathrm{f} = R_0\left[1 + \frac{a\exp(-E_\mathrm{A}/RT)t}{R_0^n}\right]^{1/n} \tag{3}$$

where

$$a = 2cM_0\gamma_\mathrm{s}\cos\phi \tag{4}$$

where c is the proportionality constant, M_0 the mobility constant, γ_s the individual surface energy of the grain boundary, ϕ the angle by which two grains are separated, R_f the final grain size, R_0 the initial grain size, E_A the activation energy for grains to move to the grain boundary, R the gas constant, T the temperature of the cell, n the constant (characteristic of the electrode material).

The value of "a" is 1.141×10^{12} [20]. The value of E_A, T, R, R_0 and n is 175.5 kJ/mol, 1023 K, 8.314 J/mol, 30 nm and 3.2, respectively [20]. An empirical correlation between grain size and temperature independent exchange current, B is given by [21]

$$B = B_0 - bR_\mathrm{f}^{1/2} \tag{5}$$

where B_0 is the initial temperature exchange current, which is equal to 270 A $\mathrm{K}^{0.5}$/pa m^2. The value of b is 6.218 for TiN electrode found experimentally by Ryan et al. [21].

The relation between temperature independent exchange current, B, and power output can be found from the simulation work done in this study (see Appendix A). It is seen that as the temperature independent exchange current increases, power output also increases at a given porosity and electrode material (TiN). However, the change of power output in the cathode side is huge compared to that of anode side. Therefore, change in power output with temperature independent exchange current of anode was neglected. From the simulation of FORTRAN code, the following relation has been obtained between the power output and temperature independent exchange current (see Appendix A):

$$P_\mathrm{e} = 1.5135 + 0.006 \times B - 10^{-5B^2} \tag{6}$$

where P_e is power output (W).

Now, for the given value of t, three Eqs. (3), (5) and (6) can be solved for three unknowns namely P_e, B and R_f. This gives the relation between the power output and time. We define this relation as simulated relation between power output and time.

4. Comparison of the experimental and empirical relations between the power output and time

Once both the experimental and simulated relations between the power output and time were found, a comparison is made between these two. An empirical relation between the power output with time (which was found after solving Eqs. (3), (5) and (6)) bears the assumption that degradation of the power output is only due to the degradation of the electrode and the degradation of the electrode is only due to the grain growth and surface self-diffusion effects. However, experimental relation between the power output and time does not necessarily assume the same assumption. The factors which had affected this experiment are degradation of electrode, electrolyte, condenser,

Table 1

	Grain size (nm)	Temperature independent exchange current (A $K^{0.5}$/Pa m^2)	Simulated power output (W)
Initial value	30	270	2.48
Final value after 15 years	368.38	150	2.21
Total change	338.38	120	0.27
Change (%)	1127.9	44.44	10.88

evaporator, cell length and cell wall, and heat losses such as, conduction heat loss, radiation heat loss, and electric internal losses such as BASE ionic resistance and the charge exchange polarization loss on the cathode side. Comparing the amount of power degradation at a certain time from both relations, the impact of the electrode degradation on overall power degradation of the AMTEC can be found.

5. Results and discussions

From the simulation, it is seen that grain size of TiN electrode increased from an initial radius of 30–368.38 nm over a 15 years of period, which is 12.28 times the initial grain radius. Temperature independent exchange current decreased from its initial value of 270–150 A $K^{0.5}$/Pa m^2. The decrease in exchange current is 44.44% over 15 years of operating time. See Table 1.

The solution of Eqs. (3), (5) and (6) gave the power output with time. The degrading factors in this simulated relation of power output with time are grain growth effects and surface self-diffusion of TiN electrode. Comparing the experimental power output and simulated power output with time, the extent of electrode degradation on the overall power degradation of AMTEC is calculated.

Comparing experimental data and the simulated results, it is seen that the power decreased from 2.48 to 1.52 W in the experimental data whereas power decreased from 2.48 to 2.3 W in the simulation results both after 12,000 h of AMTEC operation. From these numerical figures, it is concluded that the electrode is 18.75% responsible for the overall power degradation (see Appendix B). Again comparing the experimental and simulation results at the end of 18,000 h of AMTEC operation, it is seen that the power decreased from 2.48 to 1.27 W in the experimental data whereas power decreased from 2.48 to 2.29 W in the simulation results. From these numeric figures, the electrode is found to be 15.70% responsible for overall power degradation (see Appendix B). Both of these results indicate that the degradation of electrode is less than the degradation of the other components of AMTEC from 12,000 to 18,000 h of AMTEC operation.

The plots of grain growth, temperature independent exchange current, and power output (both experimental and simulated) with time for TiN electrode are shown in Figs. 2–4.

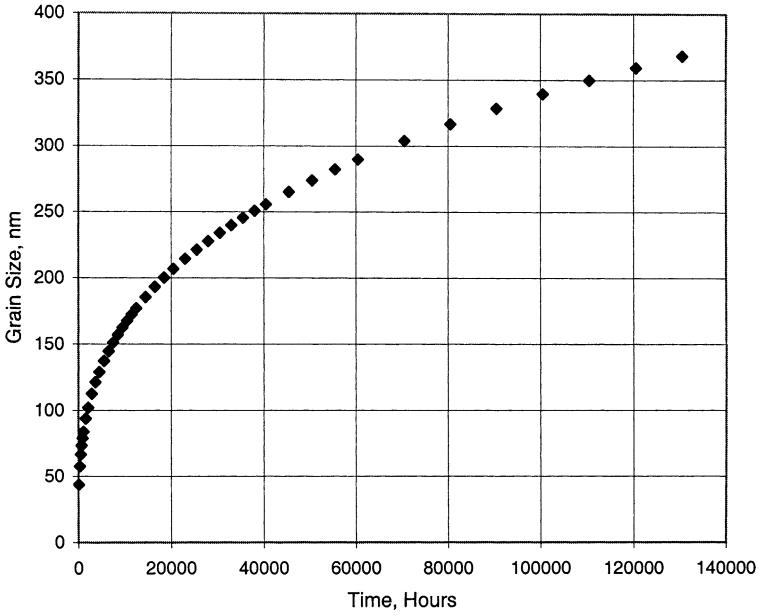

Fig. 2. The variation of grain size with time for TiN electrode.

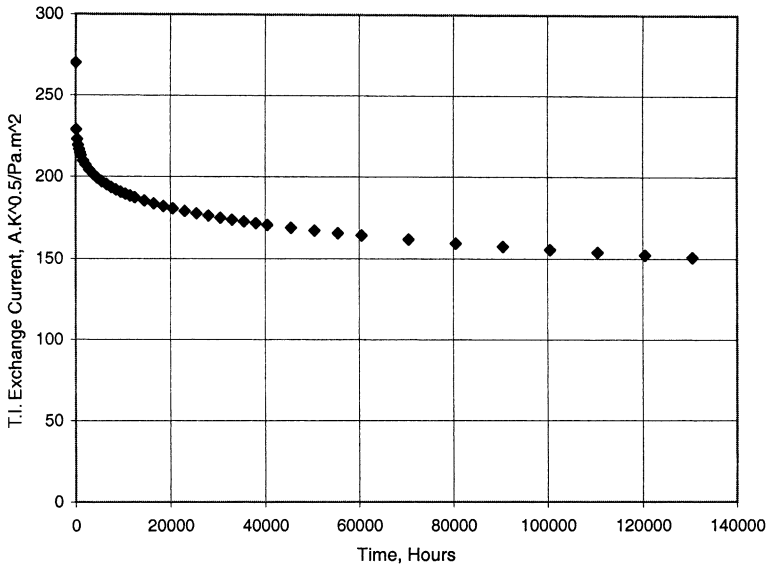

Fig. 3. The variation of temperature independent exchange current with time for TiN electrode.

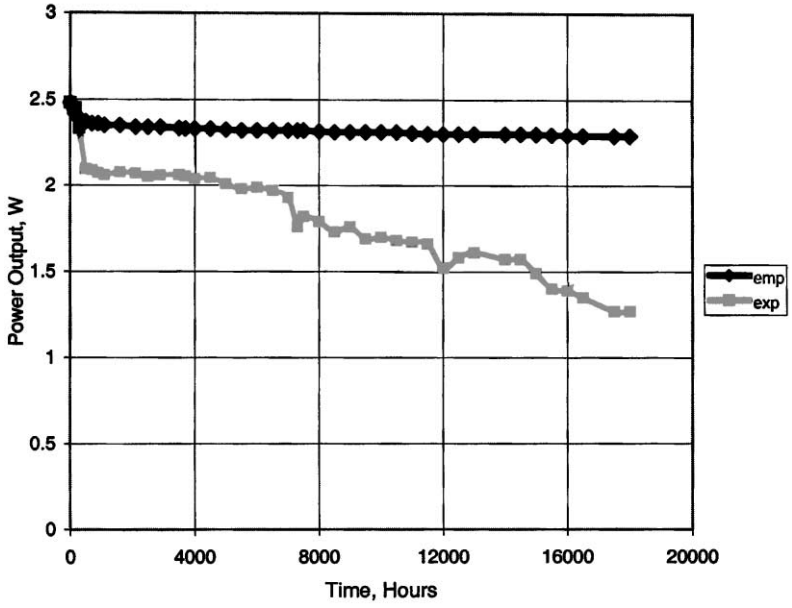

Fig. 4. Experimental and empirical power output with time for TiN electrode.

6. Conclusions

There are many components in AMTEC which have certain effective lifetime. Recent work by Vijayaraghavan [22], has shown that BASE is responsible for 50–60% of overall power degradation of AMTEC. The role of the electrode on the overall power degradation of AMTEC is similar to that of BASE but by lesser degree. Each electrode material has an effective life after which the output of the electrode does not comply with the minimum requirement of the power output of AMTEC. From this study, electrodes are found to be second most degrading components of AMTEC after BASE, whose properties change with time. The main reasons for the electrode degradation are its grain growth effect and surface self-diffusion. At the high AMTEC operating temperature range (500–1200 K), the sintering occurs in the electrode and grains of the electrode coalesce. Hence, the number of grains decreases which leads to the less contact between the electrode and electrolyte. As the number of grain decreases, the volume of grain increases and void in the electrodes starts building up. This void building phenomenon has two opposing effects. As the porosity

increases, mass transport of sodium vapor also increases leading to the increase in the power output but again electrical conductivity starts decreasing. Between these two effects, latter effect is more pronounced as time goes by. At some point voids in the electrode material get so large that there will be no apparent grain-to-grain conduction and operating lifetime of electrode is ceased.

From this analysis, it is observed that electrode is 18.75% responsible for the overall degradation after 12,000 h and 15.70% responsible for the overall degradation after 18,000 h of AMTEC operation (see Appendix B).

Acknowledgements

We are indebted to John Merrill for providing the AMTEC data before publication. This work is based in part upon work supported by the Texas Higher Education Co-ordinating Board Advanced Technology Program under Grant number 003644-091 and AFOSR sub-contract 99-08: CFDA #12,800.

Appendix A

A simulation study has been set-up with an 18,000 line FORTRAN code to study the impact of power output of AMTEC with its different parameters. The description of the simulation is given in the introduction section of this paper. From the simulation, it is seen that the power output increases with the increase of temperature independent exchange current of cathode. The plot between the power output and temperature independent exchange current is given by

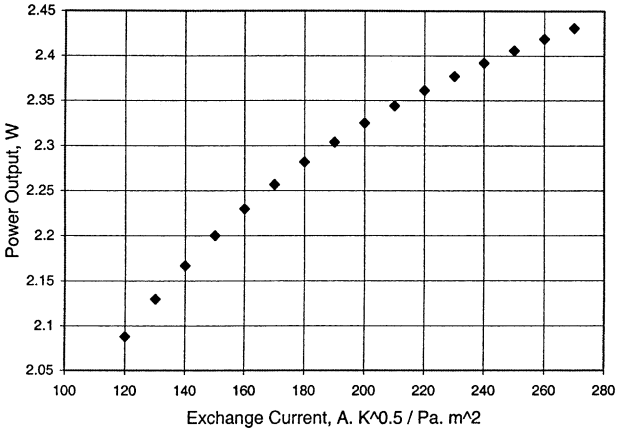

Appendix A: The Variation of Power Output with Temperature Independent Exchange Current.

From the plot, the following relation has been obtained between the power output and temperature independent exchange current which is given by

$$P_e = 1.5135 + 0.006 \times B - 10^{-5B^2}$$

where P_e is power output (W), B the temperature independent exchange current.

Appendix B. Calculation of percentage electrode (tin electrode) responsibility on the overall power degradation of AMTEC

From Fig. 4, power output at the 0 h of AMTEC operation is 2.48 W. Experimental power output after 12,000 and 18,000 h of AMTEC operation are 1.52 and 1.27 W, respectively. Total experimental power output degradations after 12,000 and 18,000 h of AMTEC operation are 0.96 and 1.21 W, respectively. These two numeric figures are the total power output degradation at that point of time.

From the same figure, power outputs of AMTEC (when only electrodes are responsible) are 2.3 and 2.29 W, respectively, after 12,000 and 18,000 h of operation. Therefore, power degradations by electrodes are 0.18 and 0.19 W, respectively, after 12,000 and 18,000 h of operation.

After 12,000 h of operation, percentage of electrode responsible on the overall power degradation $= 0.18/0.96 \times 100 = 18.75\%$.

After 18,000 h of operation, percentage of electrode responsible on the overall power degradation $= 0.19/1.21 \times 100 = 15.70\%$.

References

[1] T.K. Hunt, N. Weber, T. Cole, Research on the sodium heat engine, in: Proceedings of the 13th Intersociety Energy Conversion Engineering Conference, SAE, Warrendale, PA, 1978, p. 2011.
[2] R. Mital, Performance Evaluation of Gas Fired AMTEC Power Systems, Advance Modular Power Systems, Inc., USA, 1998, pp. 1–2.
[3] M.A. Ryan, et al., Directly deposited current collecting grids for alkali metal thermal-to-electric converter electrodes, J. Electrochem. Soc. 142 (1995) 4252–4256.
[4] M.L. Underwood, et al., Performance projections of alternative AMTEC systems and devices, American Institute of Physics, Vol. 910116, 1991, pp. 472–473.
[5] R.K. Sievers, C.P. Bankston, Radioisotope powered alkali metal thermoelectric converter design for space systems, in: D.Y. Goswami (Ed.), The American Society of Mech. Eng. 3 (1988) 159–161, Proceedings of the 23rd IECEC, 1988, p. 3.
[6] R. Mital, R.K. Sievers, J.R. Rasmussen, T.K. Hunt, Performance Evaluation of Gas Fired AMTEC Power Systems, Advance Modular Power Systems, Inc, USA, 1998, pp. 1–2.
[7] M.A.K. Lodhi, M. Schuller, P. Hausgen, Mathematical Modelling for a Thermionic-AMTEC Cascade System, Space Technology and International Forum, American Institute of Physics, 1996, pp. 1285–1290.
[8] A. Mustafa, Optimization of AMTEC-TIEC Cascade and Analysis of the Algorithm Used for Solving the Non-Linear System of Equations in the Thermal Model, Master Thesis, Texas Tech University, Vols. 1–3, 1999, pp. 20–22.
[9] V.R. Malka, Optimization of the TIEC/AMTEC Cascade Cell, Master Thesis, Texas Tech University, 1998, pp. 1–17.
[10] T.K. Hunt, R.K. Sievers, A.C. Patania, in: M.S. El-Genk (Ed.), Small AMTEC Systems as Battery Substitutes, Space Technology and

Applications International Forum, American Institute of Physics, 2000, pp. 1356–1360.
[11] T. Cole, Thermoelectric energy conversion with solid electrolytes, Science 221 (1983) 915–920.
[12] R.K. Sievers, R.F. Wright, High power density alkali metal thermal to electric converter, in: Proceedings of the 25th Intersociety Energy Conversion Engineering Conference, Vol. 2, 1990, p. 426.
[13] M.S. Chowdhury, Simulation and Analysis of the Role of the Electrodes in Power Degradation of AMTEC, Master Thesis, Texas Tech University, 2000, pp. 12–21.
[14] M.L. Underwood, et al., An AMTEC Vapor–Vapor, Series Connected Cell, American Institute of Physics, Vol. 920104, 1992, pp. 1331–1336.
[15] J.M. Tourier, M.S. El-Genk, Sodium vapor flow regimes and pressure losses on cathode side of multi-tube AMTEC cell, in: Proceedings of the 15th Symposium on Space and Nuclear Power and Propulsion, 3rd Space Technology and Application International Forum, Albuquerque, NM, American Institute of Physics, New York, 1998, pp. 2–6.
[16] J.M. Tournier, et al., An Analytical Model for Liquid-Anode and Vapor-Anode AMTEC Converters, American Institute of Physics, New York, Vol. 3, 1997, pp. 1543–1552.
[17] J.M. Tourier, M.S. El-Genk, An analysis of AMTEC, multi-cell ground-demo for the Pluto/Express Mission, in: Proceedings of the Intersociety Engineering Conference on Energy Conversion, Vol. 2, 1998.
[18] R.M. Williams, et al., Mass transport, charge transfer, and ohmic losses in the alkali metal thermoelectric converter, I. Chem. E. Sym. 112 (1989).
[19] R.M. Williams, et al., Kinetics and transport at AMTEC electrodes — I. The interfacial impedance model, J. Electrochem. Soc. 137 (1990) 1709–1715.
[20] V.B. Shields, et al., in: Proceedings of the Intersociety Energy Conversion Engineering Conference on Model for Grain in AMTEC Electrodes, New York, 1999, pp. 1–3.
[21] M.A. Ryan, et al., in: M.S. El-Genk (Ed.), Lifetimes of AMTEC Electrodes: Molybdenum, Rhodium-Tungsten, and Titanium Nitride, Space Technology and Applications International Forum, Vol. 2, 2000, pp. 1377–1382.
[22] P. Vijayaraghavan, Power Degradation and Performance Evaluation of BASE in AMTEC, Master Thesis, Texas Tech University, 2000, pp. 93–100.